CHAPTER 35

Traditional Radiology, Computed Tomography, and Magnetic Resonance Imaging in Critical Care Nephrology

Roberto Pozzi Mucelli and Matteo Catania

OBJECTIVES

This chapter will:

1. Explain indications and contraindications for computed tomography and magnetic resonance imaging in critical care nephrology.
2. Describe the technique of examination in renal computed tomography and magnetic resonance imaging.
3. Analyze the development of functional magnetic resonance.

Diagnostic imaging modalities in critical care nephrology include traditional radiology, ultrasonography, computed tomography (CT), and magnetic resonance imaging (MRI). Among these modalities, ultrasonography plays a major role in the initial workup of acute renal failure. The role of ultrasonography is illustrated and discussed in another chapter of this book.

Traditional radiology has a minor role in acute renal failure because intravenous urography has been replaced today, after the introduction of modern multislice CT scanners, by CT urography. Therefore this chapter is dedicated primarily to CT and MRI.

COMPUTED TOMOGRAPHY

Unenhanced CT is, in many cases, the only possible examination in patients with AKI, unless immediate dialysis is performed after the contrast-enhanced CT examination. In unenhanced studies, morphologic features to assess are the long axis (measured on coronal reconstruction) and the anteroposterior axis (visible on axial scans) of the kidney, the presence of calcifications (vascular, lithiasis-related, parenchymal), the parenchymal width (mean value calculated from at least three measurements), the presence of a mass (solid or cystic), and the condition of the urinary

tract. Basal CT adds clinically important information in the majority of patients with indeterminate sonograms: in acute kidney injury (AKI) patients being screened for obstruction, it can be sensitive as ultrasonography (US) in detecting hydronephrosis and much more sensitive in detecting ureteral calculi. Dilated ureters usually can be traced to the point of obstruction. Regular greyscale US is not accurate in the minimally dilated obstructive situation, such as retroperitoneal metastatic tumor or idiopathic retroperitoneal fibrosis (Fig. 35.1), in which the ureter encasement interferes with peristalsis.[1] Thus, if US cannot determinate the cause of the obstruction, nonenhanced CT can be obtained.[2] CT can show other causes of obstruction, such as neoplastic condition at the level of retroperitoneum and in the pelvis, although these are not common causes of acute kidney injury (AKI).

Nephrotoxicity of iodinated contrast agents is an important clinical problem in a patient with renal insufficiency. AKI induced by iodinated contrast media accounts for about 10% of hospital cases of renal failure, especially in azotemic patients. Indeed, excretory urography, contrast-enhanced CT, and angiography should be performed in azotemic patients only when US, unenhanced CT, and MRI are not available or their results are questionable. Nonionic, low-osmolarity or iso-osmolarity contrast media must be used because they have been demonstrated in randomized studies to be statistically less nephrotoxic than ionic contrast media in patients with normal renal function and with renal insufficiency.[3] However, the problem of contrast-induced nephrotoxicity is less critical today than in the past because the availability of modern multislice CT allows the use of less amount of contrast media to be injected. Furthermore, contrast media in CT are injected intravenously, and this route is associated rarely with contrast-induced nephrotoxicity compared with the arterial route of injection.

Contrast administration allows delineation of the main renal arteries from the point of origin up to that of secondary branching, in the cortical phase during the passage of contrast within the glomerular and peritubular capillaries, and of the main veins; in the parenchymal phase during the diffusion of contrast within interstitial extracapillary tissue and filtration through the glomerular membrane with opacification of renal tubules; and finally, the excretory system that is depicted, in normal functioning kidneys, at 3 to 4 minutes after contrast administration, the peak being reached after 10 to 15 minutes.[4]

Contrast-enhanced CT is much more reliable than excretory urography in detecting structural deformities of the nephrogram and requires less contrast material. In spite of a few differences, all the urographic signs have their counterpart in contrast-enhanced CT. For these reasons excretory urography is no longer performed, and it has been replaced by CT urography. However, excretory urography and CT urography have a limited role in patients with AKI because iodinated contrast agents may exacerbate the existing renal failure.

In acute renal obstruction an early cortical nephrogram develops followed by gradual opacification of the medulla. Delay in opacification of the pyelocalyceal system and hydronephrosis are appreciable. The cause of obstruction, either intrinsic or extrinsic, usually is identified (Fig. 35.2).

In acute bacterial nephritis wedge-shaped lesions, focal mass-like lesions, or diffuse, multifocal mass-like lesions leading to abscess formation are appreciable depending on the severity of the disease (Fig. 35.3). In patients with cortical necrosis, opacification of the renal cortex is lacking. They

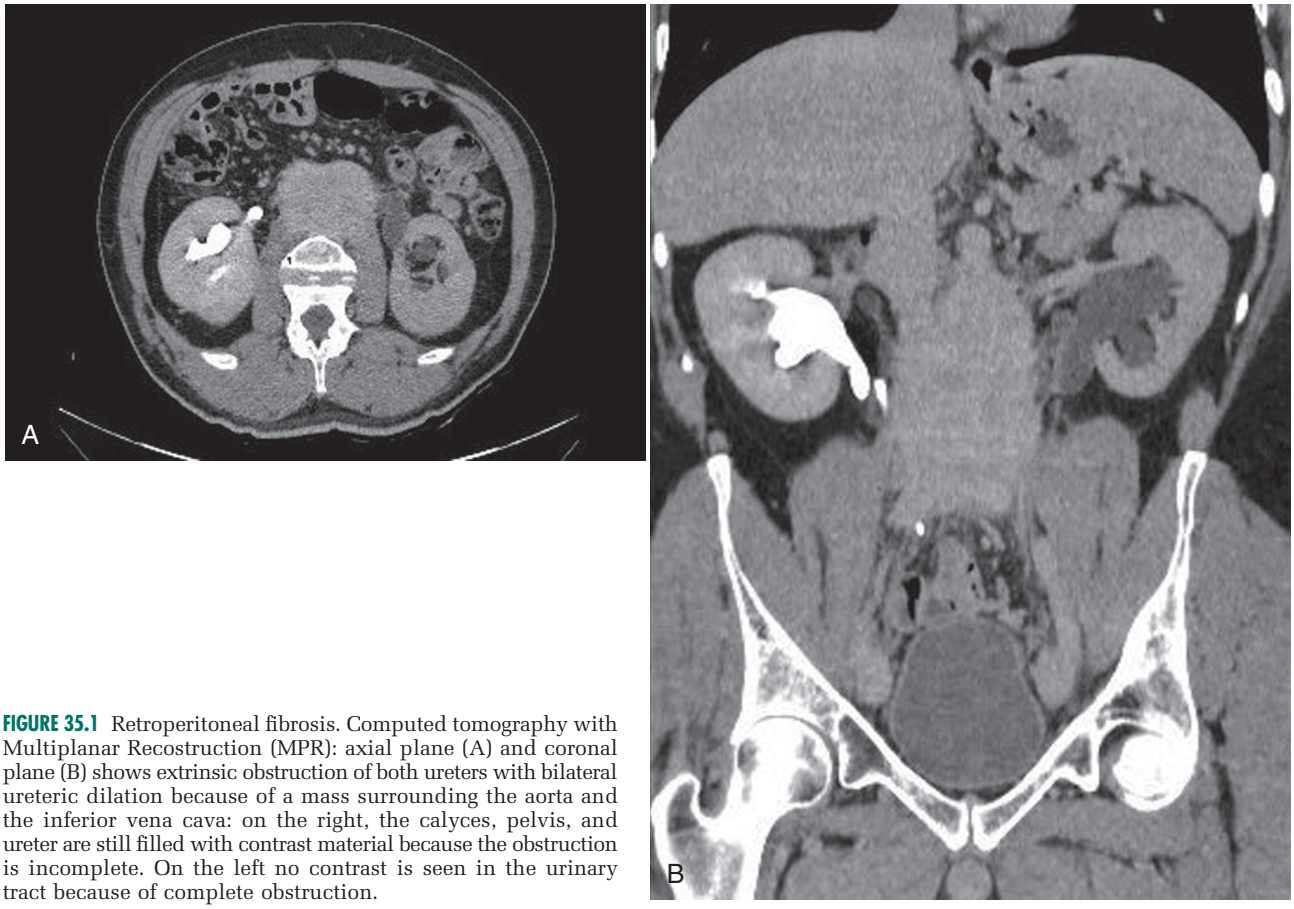

FIGURE 35.1 Retroperitoneal fibrosis. Computed tomography with Multiplanar Recostruction (MPR): axial plane (A) and coronal plane (B) shows extrinsic obstruction of both ureters with bilateral ureteric dilation because of a mass surrounding the aorta and the inferior vena cava: on the right, the calyces, pelvis, and ureter are still filled with contrast material because the obstruction is incomplete. On the left no contrast is seen in the urinary tract because of complete obstruction.

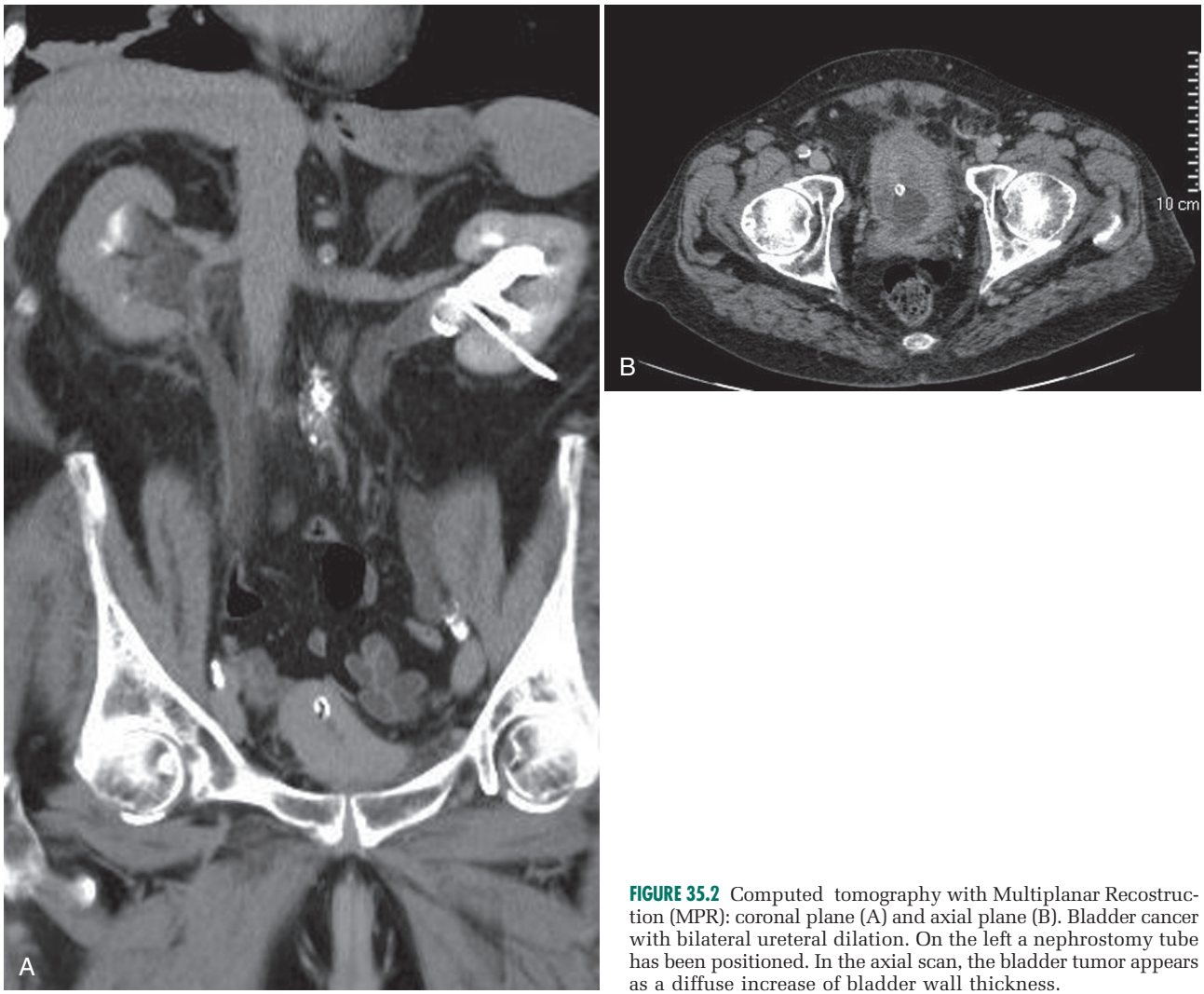

FIGURE 35.2 Computed tomography with Multiplanar Recostruction (MPR): coronal plane (A) and axial plane (B). Bladder cancer with bilateral ureteral dilation. On the left a nephrostomy tube has been positioned. In the axial scan, the bladder tumor appears as a diffuse increase of bladder wall thickness.

present subcapsular, juxtamedullary, and medullary enhancement without excretion of the contrast medium.[3]

MAGNETIC RESONANCE IMAGING

MRI produces comparable image quality of the kidney to CT. Magnetic resonance (MR) sequences provide information about tissues, including T1 and T2 relaxation times, lipid or fat content, and enhancement characteristics of tissues. MRI provides versatile and unique soft tissue contrast and allows the evaluation of a wide range of urinary tract disorders. This result can be obtained by the intensity of the static magnetic field (actually from 1.5 to 3 Tesla), gradient quality and intensity, multichannel phased-array coils, advance pulse sequences, parallel imaging techniques, fast sequences, and gadolinium-based contrast agents. MRI in AKI allows evaluation of morphologic and functional changes and, in contrast with CT, can be performed without contrast or with smaller amounts of contrast with less nephrotoxicity. However, development of systemic nephrogenic fibrosis after gadolinium administration in a patient with renal failure is a well-known problem, which has limited this clinical application in patients with renal failure, acute and chronic.[5]

Usually, MRI of the kidneys is obtained on the axial and the coronal planes with breath-hold sequences. Another way to reduce respiratory motion artifacts is to use a respiratory triggering technique. This technique allows use of shorter echo train length, more signal averaging, and higher spatial resolution, without being restricted by breath-hold time. This approach can result in a higher signal-to-noise ratio (SNR) in comparison with breath-hold approaches.

The renal parenchyma is composed of two distinct zones, the cortex and medulla. Because the renal cortex presents lower T1- and T2- relaxation times in comparison with the renal medulla, the two zones can be distinguished. Anyway, renal corticomedullary image contrast is usually more conspicuous on T1-weighted images. On T1-weighted sequences, the renal cortex appears brighter than the renal medulla, whereas on T2-weighted sequences, the renal cortex appears slightly less intense than the renal medulla. The renal pelvis containing fat appears hyperintense on T1- and T2-weighted sequences. When fat-suppressed MRI sequences are employed, the fat appears hypointense on T1- and T2-weighted sequences.

T1 sequences without contrast provide more structurally defined morphologic information than that obtainable using unenhanced CT, although spatial resolution is lower with MRI. T2 sequences are used only without contrast, because gadolinium, at low concentration, does not affect T2

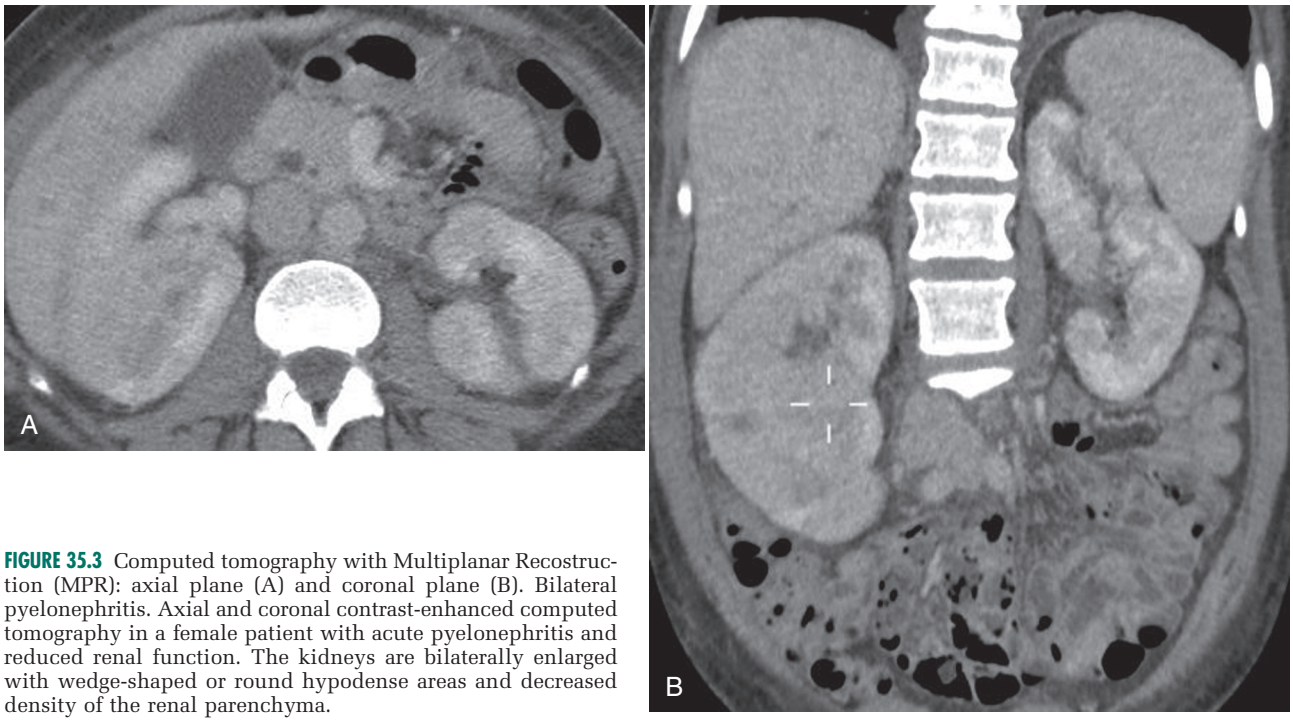

FIGURE 35.3 Computed tomography with Multiplanar Recostruction (MPR): axial plane (A) and coronal plane (B). Bilateral pyelonephritis. Axial and coronal contrast-enhanced computed tomography in a female patient with acute pyelonephritis and reduced renal function. The kidneys are bilaterally enlarged with wedge-shaped or round hypodense areas and decreased density of the renal parenchyma.

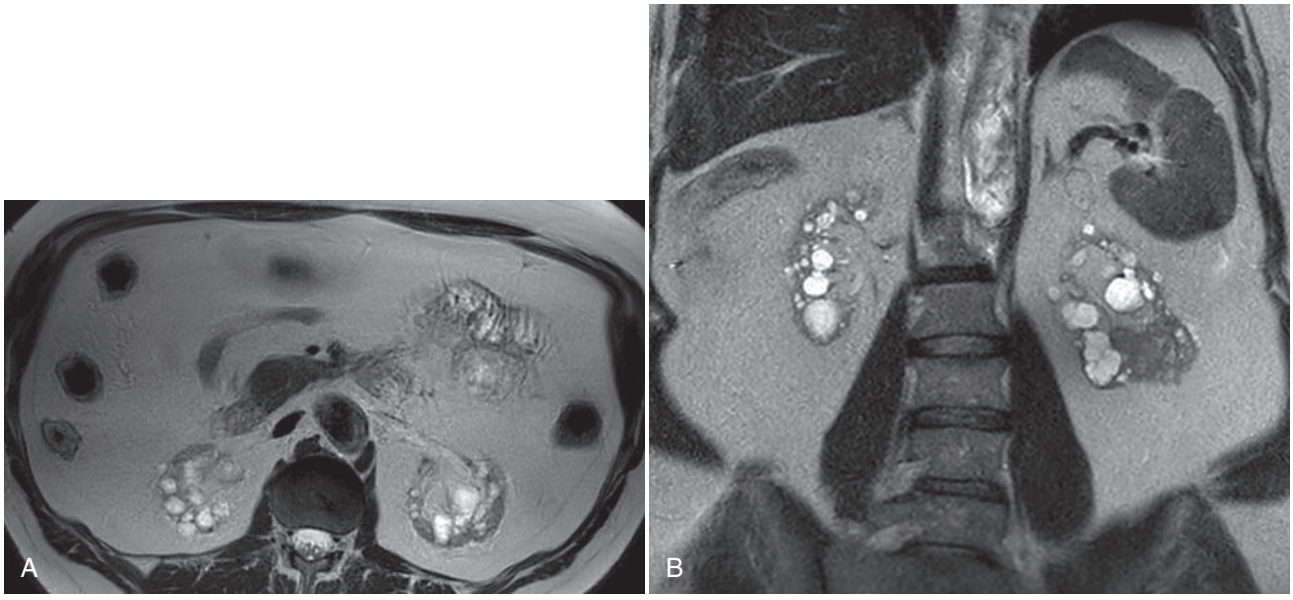

FIGURE 35.4 Magnetic Resonance Imaging: Half-Fourier-Acquired Single-shot Turbo spin Echo (HASTE): axial plane (A) and coronal plane (B). Bilateral pyelonephritis. Axial and coronal contrast-enhanced computed tomography in a female patient with acute pyelonephritis and reduced renal function. The kidneys are bilaterally enlarged with wedge-shaped or round hypodense areas and decreased density of the renal parenchyma.

relaxation time. They provide less anatomic details than is possible with T1 sequences but present better definition, allowing evaluation of the normal and pathologic structure of the kidney. With dedicated T2-weighted sequences, it is possible to examine the urinary tract, especially if dilated, allowing the generation of images from static fluid (by means of magnetic resonance urography performed without contrast) (Figs. 35.3 and 35.4).[6]

The kidneys are represented optimally in the different acquisition planes: transverse, coronal, and sagittal. The coronal plane allows good visualization of both kidneys and the relationships with the adjacent anatomic structures. Morphologic evaluation consists of definition of the long diameter of both kidneys and the parenchymal width, with visualization of the cortex, as well as a corticomedullary differentiation. It is also possible to differentiate the peripheral from the central cortex.

Altered corticomedullary relationship is recognized frequently in patients with AKI and acute renal diseases by using T1-weighted sequences. However, these changes are not specific.

In suspected postrenal AKI, MR urography is valuable in assessing hydronephrosis and detecting the cause and the site of obstruction. MR angiography is also useful in assessing

abnormalities of renal artery and vein. MR angiography usually is performed with contrast enhancement, following intravenous injection of gadolinium chelates. However, in recent years, a number of advanced non–contrast-enhanced "angiographic" pulse sequences have been introduced on modern equipment, which allow comparable image quality of renal arteries with the conventional contrast-enhanced MR angiographic images. These new sequences without the use of gadolinium are of interest mainly in patients with renal failure because the risk of nephrogenic systemic fibrosis is avoided completely.

FUNCTIONAL MAGNETIC RESONANCE IMAGING

In clinical practice, serum creatinine (SCr) levels are used for the routine diagnosis and staging of AKI because of the relative simplicity and convenience of the test. However, the SCr level has major limitations as a biomarker for AKI. First, it does not change until approximately 50% of kidney function is lost. Therefore it is not sensitive to the rapid changes in renal function induced by AKI. Moreover, the lag time between renal injury and the increase in the SCr level results in missed therapeutic opportunities, which may be responsible for the high mortality associated with AKI. Second, the SCr level depends on many other factors, such as muscle mass, age, sex, medications, and hydration status. Thus a better understanding and early detection of AKI are important for its treatment.[7]

With the development of MRI, use of functional renal MRI has grown rapidly and could be used to evaluate renal morphology and function noninvasively and simultaneously. A number of advanced MR techniques have been proposed, such as dynamic contrast-enhanced MRI (DCE-MRI), blood oxygen level–dependent (BOLD) imaging, arterial spin labeling (ASL), and diffusion-weighted imaging (DWI). These approaches can provide information on intrarenal oxygenation, perfusion, and diffusion on a microstructural level, which may not only allow the noninvasive detection of the presence and severity of renal abnormalities associated with AKI in preclinical setting but also demonstrate the pathophysiology and progress of AKI.

Dynamic Contrast-Enhanced Magnetic Resonance Imaging

Paramagnetic contrast agents (based on gadolinium [Gd]) are used with T1-weighted sequences. With use of ultrafast techniques, they allow the acquisition of data to provide high-resolution anatomic detail and functional data. As with CT, it is possible to study the various phases of contrast passage of the vascular, parenchymal, and excretory levels: after the intravenous administration of gadolinium-based contrast agents, the vascular corticomedullary phase begins immediately after the contrast medium reaches the kidneys. The nephrographic phase begins 60 to 90 seconds after contrast administration. The excretory phase begins 2 minutes after contrast administration with evidence of contrast excretion in the collecting system. Fat saturation sequences eliminate the high-intensity signals from fat tissue that interfere with interpretation of the post–contrast-enhanced images, thereby improving the quality of the study.

Changes of the signal intensity curve measured in the medulla were detected in dogs with experimentally induced AKI, and alteration of the signal intensity curve was demonstrated in the pyelocaliceal system of patients with renal failure. However, these findings are nonspecific and can be observed in a wide series of patients with acute and chronic renal impairment.[3]

Although DCE-MRI with low Gd dose is capable of measuring single-kidney GFR with higher accuracy than serum creatinine, it is typically not used for assessing AKI because lowered GFR in severe AKI patients potentially could increase the risk of NSF. In fact, the gadolinium-related nephrogenic systemic fibrosis has limited clinical applications of DCE-MRI.[8]

Blood Oxygen Level–Dependent Magnetic Resonance Imaging

BOLD MRI measurements are based on changes in the magnetic properties of hemoglobin that accompany its conversion from oxyhemoglobin to deoxyhemoglobin. Deoxyhemoglobin generates a magnetic moment because of its unpaired iron electrons. Increased deoxygenated hemoglobin concentrations lead to alterations in the magnetic spin properties of neighboring water molecules, which speeds up magnetic spin dephasing and decreases signal intensity on apparent spin–spin relaxation time-weighted (T2) MRIs. The rate of magnetic spin dephasing, R2* (=1/T2), is a measure of the tissue content of deoxygenated hemoglobin, which in turn reflects tissue oxygen partial pressure (pO_2). A decrease in R2* implies decreased deoxygenated hemoglobin concentration and increased tissue pO_2.[9] A strong correlation has been proven between renal BOLD MRI to tissue oxygen pO_2.[11] The pathophysiology of AKI is not yet fully understood, but renal tissue hypoperfusion and hypoxia are well accepted to be closely related to the pathophysiology of all forms of AKI.

In pig models of AKI induced by acute renal ischemia, the R2* values of the cortex and medulla both increased, which demonstrated a reduction in intrarenal oxygenation in parallel with decreased intrarenal blood flow during acute ischemia. After reperfusion, the intrarenal oxygenation levels immediately return to baseline oxygenation, which demonstrated that some of the early changes in renal oxygenation resulting from AKI may reverse.[12,13] Furthermore, the degree of ischemic reperfusion injury commonly influences the recovery of renal function.[14]

BOLD MRI also has been used to study the mechanisms of contrast-induced AKI. It is indicated that the administration of contrast agent caused an early and transient decrease in the medullary R2* followed by a sustained increase above the baseline in animal models of contrast-induced AKI, whereas minimal changes were observed in the renal cortex.[15,16] The differences in the variations in R2* between the renal medullary and cortex agree with the basis of renal pathophysiology. Specifically, most of the oxygen consumed by the kidney is due to the reabsorption of filtered sodium by the medulla thick ascending limb of the loop of Henle, but only approximately 5% of renal blood flow is supplied to the medulla, which makes it more susceptible to hypoperfusion and hypoxia. However, conflicting mechanisms of the initial decrease in the medullary R2* after a contrast agent injection have been reported, and a consensus has not been reached.

Li et al.[16] demonstrated that the immediate increase in R2* in the renal inner stripe of the outer medulla (ISOM) after the injection of a contrast agent may be the earliest biomarker of AKI. In addition, the effects of some interventions to mitigate the adverse effects of contrast media have

been evaluated using BOLD MRI, and the results showed that the rate of increase in R2* in the renal ISOM can be reduced by treatment with furosemide (diuretic) or N-acetylcysteine (NAC; antioxidant) before contrast media injection, but the optimum dose of furosemide and NAC for mitigating the negative effects of contrast media has not yet been determined.[17]

Renal oxygenation in AKI resulting from other causes, such as sepsis-associated AKI and other nephrotoxin-induced AKI, also has been studied in several experimental animal models and humans using BOLD MRI.[18,19]

In conclusion, BOLD MRI not only can noninvasively assess changes in renal oxygenation resulting from AKI by measuring the R2* levels of the renal cortex and medulla but also can investigate the role of hypoxia in the pathogenesis and progress of AKI.[7] In recent years, this strategy has been used to assess AKI, but currently its clinical application in AKI is still marginal because of the limited availability of MRI scanners, already employed in other fields. Moreover, further studies are necessary to establish the cutoff R2* values for the diagnosis of AKI and evaluate the specificity of R2* for the renal oxygenation status.[7]

Arterial Spin Labeling

ASL is a novel, noninvasive MRI technique used to measure tissue perfusion, that is, tissue blood flow,[20] by magnetically labeled water protons in the blood as an endogenous contrast agent. First, the water in the blood is labeled before it enters the tissue of interest. The labeled water then flows into tissue and is exchanged with tissue water, thereby altering its magnetization. The perfusion-weighted image is obtained by subtracting the labeled image from a control image with unlabeled blood water to obtain the difference, and the signal intensity is proportional to perfusion. Finally, a kinetic model is used to directly quantify perfusion if other parameters, such as the tissue T1 relaxation time, blood-tissue partition coefficient, and transit time of the blood water to tissue water, are known.[7]

Dong et al.[21] performed a pilot study to demonstrate the feasibility of ASL perfusion MRI in the detection of AKI and found that the cortical, medullary, and global kidney blood flows were significantly lower in AKI patients than in healthy volunteers. This finding suggested that the decrease in renal perfusion is critical to the pathophysiology of AKI, which is in agreement with previous reports on the basis of the evaluation of renal blood flow of AKI.[22-24] Furthermore, ASL also was shown to be able to noninvasively detect the severity of AKI and monitor renal perfusion impairment over time in a mouse model of ischemia-induced AKI. The degree of perfusion impairment measured using ASL is related to kidney volume loss, the severity of histopathologic alterations of renal tissue, and the impairment of renal function. In addition, renal perfusion measured by means of ASL also may serve as a noninvasive biomarker to predict the extent of subsequent histologic alterations of the kidney early after the organ is damaged. Thus ASL may be very valuable for the clinical follow-up of patients who are at risk for AKI and for drug development in experimental renal disease models.[25]

Zimmer et al.[26] reported that ASL is a valid alternative to DCE-MRI, and ASL may be preferred for patients with impaired kidney function because the injection of Gd-based contrast agents may cause nephrogenic systemic fibrosis.

However, the relatively low SNR and short signal decay rate of the ASL technique will delay its clinical application. A high-field MR scanner (at least 1,5 T) is necessary to enhance the image quality and provide a more accurate analysis of renal perfusion using the ASL technique.[27]

Diffusion-Weighted Imaging

DWI is a powerful technique that provides information on the renal microstructure and function by characterizing water motion on a molecular level.[28,29] The apparent diffusion coefficient (ADC) is used as a quantitative parameter of diffusion, which is calculated from DWI images with a monoexponential decay model. Structural changes, such as interstitial fibrosis or tubular atrophy, could result in a decrease in the ADC value, which has been demonstrated to correlate with renal function. Renal diffusion in healthy and disease states has been evaluated using this technique.[28] In a mouse model of ischemia-induced AKI, the ability of the DWI value to characterize acute and chronic pathology after unilateral AKI was investigated. The ADC value of the renal medulla was shown to be significantly decreased at every time point after AKI, and the renal ADC values changed with the severity of AKI and the degree of interstitial renal fibrosis 4 weeks after AKI. This finding suggested that the decrease in renal diffusion is critical to the pathophysiology of AKI, which is associated with renal tissue edema, inflammatory cell infiltration, and subsequent development of interstitial renal fibrosis and tubular atrophy.[10]

Nevertheless, the ADC values, which derive from the conventional monoexponential model, provide a mix of information on capillary perfusion and water diffusion in the extravascular space.[30]

In summary, capabilities and parameters of major MRI techniques are

- Dynamic contrast-enhanced MRI (DCE MRI): tracer transit through vascular space and tubules; it values GFR, perfusion, vascular and tubular mean transit times (MTT)
- Blood oxygen level–dependent (BOLD): direct measure of deoxyhemoglobin, and reflects blood and tissue pO_2; it values spin-spin relaxation rate (R2* = 1/T2*), medulla-cortex R2*ratio (MCR =R2*Med/R2*Cx)
- Arterial spin labeling (ASL): perfusion without injecting tracer; it values perfusion
- Diffusion-weighted imaging (DWI): water diffusion in interstitial space, capillary flow; it values apparent diffusion coefficient (ADC), anisotropy, perfusion fraction

In summary, functional renal imaging is a growing field of interest with great potential, particularly the BOLD, ASL, and DWI techniques, which assess the oxygenation, perfusion, and diffusion properties of the kidney. Moreover, because these techniques do not require the administration of exogenous contrast agents, they also can be applied in patients with impaired renal function. Although the lack of standardized sequences, postprocessing software, and models hinders the widespread use of these techniques in clinical settings, numerous published papers have demonstrated the feasibility of the techniques for assessing the renal pathophysiology of AKI triggered by different causes. Further improvements in the hardware and postprocessing software are essential to improve our understanding of the renal pathophysiology and progress of AKI.[7]

Key Points

1. Unenhanced computed tomography is often the only possible examination in patients with acute

kidney injury (AKI) because of nephrotoxicity of iodinated contrast agents; basal computed tomography is highly sensitive in detecting hydronephrosis and ureteral calculi.
2. Functional magnetic resonance imaging could be used to evaluate simultaneously and noninvasively renal morphology and function.

Key References

2. Ramer EM, Papanicolau N, et al. ACR Appropriateness Criteria(®) on renal failure. *Am J Med*. 2014;127(11):1041-1048, e1.
3. Pozzi Mucelli R, Bertolotto M, Quaia E. Imaging techniques in acute renal failure. *Contrib Nephrol*. 2001;132:76-91.
6. Ronco, et al. Critical Care Nephrology, ed 2. Computed Tomography and Magnetic Resonance Imaging in Acute renal Failure p.276, Philadelphia, 2009, Saunders.
7. Zhou HY, Chen TW, Zhang XM. Functional magnetic resonance Imaging in acute kidney injury: present status. *Biomed Res Int*. 2016;2016:2027370.
9. Neugarten J, Golestaneh L. Blood oxygenation level-dependent MRI for assessment of renal oxygenation. *Int J Nephrol Renovasc Dis*. 2014;7:421-435.

A complete reference list can be found online at ExpertConsult.com.

References

1. Spital A1, Valvo JR, Segal AJ. Nondilated obstructive uropathy. *Urology*. 1988;31(6):478-482.
2. Ramer EM, Papanicolau N, et al. ACR Appropriateness Criteria(®) on renal failure. *Am J Med*. 2014;127(11):1041-1048, e1.
3. Pozzi Mucelli R, Bertolotto M, Quaia E. Imaging techniques in acute renal failure. *Contrib Nephrol*. 2001;132:76-91.
4. Kawashima A1, Vrtiska TJ, LeRoy AJ, et al. CT urography. *Radiographics*. 2004;24(suppl 1):S35-S54, discussion S55-8.
5. Quaia E, et al. Radiological imaging of the kidney, ed 2. Magnetic Resonance Imaging 2.2.4 p.36.
6. Ronco, et al. Critical Care Nephrology, ed 2. Computed Tomography and Magnetic Resonance Imaging in Acute renal Failure p.276, Philadelphia, 2009, Saunders.
7. Zhou HY, Chen TW, Zhang XM. Functional magnetic resonance imaging in acute kidney injury: present status. *Biomed Res Int*. 2016;2016:2027370.
8. Zhang JL, Morrell G, Rusinek H, et al. New magnetic resonance imaging methods in nephrology. *Kidney Int*. 2014;85(4):768-778.
9. Neugarten J, Golestaneh L. Blood oxygenation level-dependent MRI for assessment of renal oxygenation. *Int J Nephrol Renovasc Dis*. 2014;7:421-435.
10. Hueper K, Rong S, Gutberlet M, et al. T2 relaxation time and apparent diffusion coefficient for noninvasive assessment of renal pathology after acute kidney injury in mice: comparison with histopathology. *Invest Radiol*. 2013;48(12):834-842.
11. Pohlmann A, Arakelyan K, Hentschel J, et al. Detailing the relation between renal T2* and renal tissue pO2 using an integrated approach of parametric magnetic resonance imaging and invasive physiological measurements. *Invest Radiol*. 2014;49(8):547-560.
12. Alford SK, Sadowski EA, Unal O, et al. Detection of acute renal ischemia in swine using blood oxygen level-dependent magnetic resonance imaging. *J Magn Reson Imaging*. 2005;22(3):347-353.
13. Juillard L, Lerman LO, Kruger DG, et al. Blood oxygen level-dependent measurement of acute intra-renal ischemia. *Kidney Int*. 2004;65(3):944-950.
14. Pedersen M, Laustsen C, Perot V, et al. Renal hemodynamics and oxygenation in transient renal artery occluded rats evaluated with iron-oxide particles and oxygenation-sensitive imaging. *Z Med Phys*. 2010;20(2):134-142.
15. Haneder S, Augustin J, Jost G, et al. Impact of iso- and low-osmolar iodinated contrast agents on BOLD and diffusion MRI in swine kidneys. *Invest Radiol*. 2012;47(5):299-305.
16. Li L-P, Lu J, Zhou Y, et al. Evaluation of intrarenal oxygenation in iodinated contrast-induced acute kidney injury-susceptible rats by blood oxygen level-dependent magnetic resonance imaging. *Invest Radiol*. 2014;49(6):403-410.
17. Li L-P, Thacker J, Lu J, et al. Efficacy of preventive interventions for iodinated contrast-induced acute kidney injury evaluated by intrarenal oxygenation as an early marker. *Invest Radiol*. 2014;49(10):647-652.
18. Hofmann L, Simon-Zoula S, Nowak A, et al. BOLD-MRI for the assessment of renal oxygenation in humans: acute effect of nephrotoxic xenobiotics. *Kidney Int*. 2006;70(1):144-150.
19. Tran M, Tam D, Bardia A, et al. PGC-1α promotes recovery after acute kidney injury during systemic inflammation in mice. *J Clin Invest*. 2011;121(10):4003-4014.
20. Williams DS, Detre JA, Leigh JS, et al. Magnetic resonance imaging of perfusion using spin inversion of arterial water. *Proc Natl Acad Sci USA*. 1992;89(1):212-216.
21. Dong J, Yang L, Su T, et al. Quantitative assessment of acute kidney injury by noninvasive arterial spin labeling perfusion MRI: a pilot study. *Sci China Life Sci*. 2013;56(8):745-750.
22. Wen X, Murugan R, Peng Z, et al. Pathophysiology of acute kidney injury: a new perspective. *Contrib Nephrol*. 2010;165:39-45.
23. Basile DP, Anderson MD, Sutton TA. Pathophysiology of acute kidney injury. *Compr Physiol*. 2012;2(2):1303-1353.
24. Singh P, Ricksten S-E, Bragadottir G, et al. Renal oxygenation and haemodynamics in acute kidney injury and chronic kidney disease. *Clin Exp Pharmacol Physiol*. 2013;40(2):138-147.
25. Hueper K, Gutberlet M, Rong S, et al. Acute kidney injury: arterial spin labeling to monitor renal perfusion impairment in mice-comparison with histopathologic results and renal function. *Radiology*. 2014;270(1):117-124.
26. Zimmer F, Zöllner FG, Hoeger S, et al. Quantitative renal perfusion measurements in a rat model of acute kidney injury at 3T: testing inter- and intramethodical significance of ASL and DCE-MRI. *PLoS ONE*. 2013;8(1).
27. Wang J, Alsop DC, Li L, et al. Comparison of quantitative perfusion imaging using arterial spin labeling at 1.5 and 4.0 Tesla. *Magn Reson Med*. 2002;48(2):242-254.
28. Notohamiprodjo M, Reiser MF, Sourbron SP. Diffusion and perfusion of the kidney. *Eur J Radiol*. 2010;76(3):337-347.
29. Le Bihan D, Turner R, Douek P, et al. Diffusion MR imaging: clinical applications. *Am J Roentgenol*. 1992;159(3):591-599.
30. Le Bihan D, Breton E, Lallemand D, et al. Separation of diffusion and perfusion in intravoxel incoherent motion MR imaging. *Radiology*. 1988;168(2):497-505.